# Planar Differential Antenna for Short-Range UWB Pulse Radar Sensor

D. Pepe, *Member, IEEE*, L. Vallozzi, H. Rogier, *Senior Member IEEE*, and D. Zito, *Member, IEEE*

***Abstract*—A novel planar differential ultra-wideband (UWB) antenna was designed and implemented on low-cost FR4 substrate and characterized experimentally. The dedicated design was motivated by the implementation of a UWB pulse radar sensor obtained by co-integrating a system-on-a-chip UWB pulse radar packaged in QFN32 package with the proposed antenna, one for the transmitter and one for the receiver. The experimental results confirm the predictions obtained by simulations, and the effectiveness of the novel antenna design for the implementation of low-cost short-range pulse radar sensor was validated by field operational tests.**

***Index Terms*— Ultra-wideband (UWB), planar antenna, differential antenna, short-range radar, biomedical applications.**

## I. Introduction

IN February 2002 the Federal Communications Commission (FCC) authorized the marketing and operation of a new class of products incorporating ultra-wideband (UWB) technology [1]. UWB devices transmit and receive extremely short radio-frequency pulses, with time duration in the range from tens of picoseconds to tens of nanoseconds. As a consequence, the frequency spectrum of the transmitted signal has very wide band occupancy (several GHz) and very low power spectral density (PSD). The maximum in-band (3.1-10.6 GHz) allowed equivalent isotropic radiated power (EIRP) spectral density is -41.3 dBm/MHz. According to the FCC definitions, a UWB system is any radio system operating in a bandwidth greater or equal to 500 MHz, or with a fractional band greater or equal to 10%, operating in the above spectrum region. This is a key enabling radio technology for several unlicensed commercial applications, such as ground penetrating radar (GPR) systems, wall and through wall imaging systems, surveillance systems, high data rate communication systems and medical imaging.

Recently the first system-on-a-chip (SoC) UWB pulse radar, operating in compliance with the FCC mask, was implemented in 90 nm CMOS technology by our research group [2]. The entire UWB pulse radar sensor was implemented by co-integrating the radar microchip above and two novel planar differential antennas (transmitting and receiving) designed and realized on FR4 substrate. This paper addresses the design, simulation and experimental characterization of the novel UWB antenna, which was not reported in our previous publications focused exclusively on the SoC implementation of the radar microchip [2], and on the functional and field operational tests for respiratory rate detections [3], whose results will be not repeated here.

The paper is organized as follows. Section II reports the description of the novel antenna design. Section III, reports the results of simulations and measurements. Finally, in Section IV, the conclusions are drawn.

## II. Antenna Design

The interest in UWB applications has stimulated a considerable number of UWB antenna designs [4, 5]). As for complete systems, recently a SoC UWB pulse radar for respiratory rate monitoring was successfully implemented in 90 nm CMOS technology and tested experimentally [2]. The radar test-chip is packaged into a QFN32 package of size 5×5 $mm^2$. The receiver input and transmitter output of the SoC UWB pulse radar were designed on the two opposite sides of the silicon die in order to allow a straightforward connection of input and output pins to the two planar antennas realized on the same board of the radar sensor, as shown in Fig. 1. The board containing two UWB antennas, one for the transmitter and one for the receiver, was designed in a low-cost FR4 substrate ($\varepsilon_R$=4.4, dielectric thickness equal to 1.6 mm, copper thickness of 35 μm, and loss tangent equal to 0.02). The antenna was simulated and optimized by means of Momentum by Agilent Technologies®. A differential topology has been adopted in accordance with the fully differential topology of receiver and transmitter of the SoC UWB radar [6, 7]. Each lobe of the antenna consists of a semicircle (radiating part) and a triangle which provide a smooth transition towards the microchip pins. The antenna terminals ($in_p$ and $in_m$ in Fig. 1) are designed in order to realize the appropriate feeding from the transmitter and to the receiver of the radar microchip pins. Overall, this approach allows a compact design of both the

Manuscript received March 4, 2013; revised October 4, 2013; accepted November 11, 2013. This work was supported in part by the Science Foundation Ireland (SFI), in part by the Irish Research Council (IRC), and in part by the Higher Education Authority (HEA).

Domenico Pepe is with the Tyndall National Institute, "Lee Maltings", Dyke Parade, Cork, Ireland.

Luigi Vallozzi and Hendrik Rogier are with the Department of Information Technology, Ghent University, Sint-Pietersnieuwstraat 41, 9000 Gent, Belgium.

Domenico Zito is with the Dept. of Electrical and Electronic Engineering, University College Cork, and Tyndall National Institute, "Lee Maltings", Dyke Parade, Cork, Ireland (email to: domenico.zito@tyndall.ie).

Color versions of one or more of the figures in this paper are available online at http://ieeexplore.ieee.org.

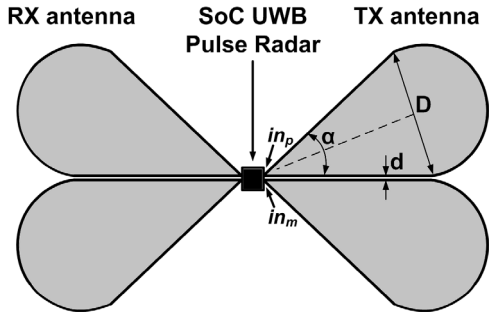


Fig. 1. Board floor-plan for the radar sensor. Two antennas (one for the transmitter and one for the receiver) were designed on two opposite sides of the board in order to facilitate the connection to the transmitter output and receiver input of the SoC UWB radar packaged in QFN32.

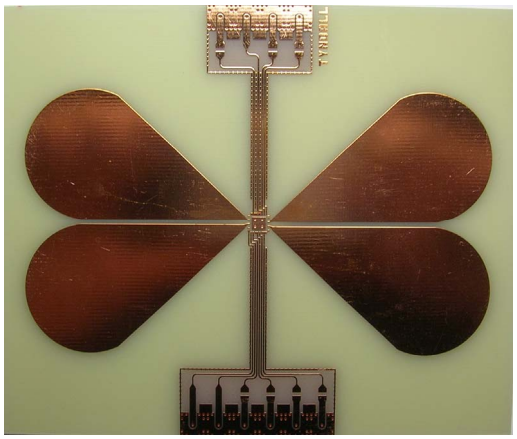

Fig. 3. Photograph of the board of the UWB radar sensor. The transmitter antenna on left and the receiver antenna on right.

transmitter and receiver antennas on the same board of the radar sensor. The distance d between the two sides of the antenna is equal to 1 mm. The diameter D is equal to 3 cm in order to resonate at the frequency of interest (i.e. about 3 GHz). The angle α is equal to 45 degrees.

The above design can't verified experimentally, since the antenna feeds have been designed in order to be connected to the radar test chip input and output pins, as shown in Fig. 3. Thereby, the design of a stand-alone version has been derived from the above design in order to verify the performance by means of the relevant direct experimental tests. The layout of the stand-alone antenna is shown in Fig. 2. Note that in the stand-alone antenna, two microstrip feeding lines were added in order to allow the connection of the antenna to a Vector Network Analyzer (VNA) by means of 2.92 mm connectors. The width of the microstrip line feeding paths ($W_P$) is equal to 3 mm in order to exibit a 50 Ω characteristic impedance. The distance $d_{in}$ between the two inputs of the antenna is equal to 1 cm to allow the placement of two adjacent connectors, as shown in Fig. 2. The characteristic sizes of the UWB antenna are reported in Table I, which are the same for both the radar sensor and stand-alone designs. In order to make explicit the link to the complete system, the letter also reports the simulation results of the on-board design.

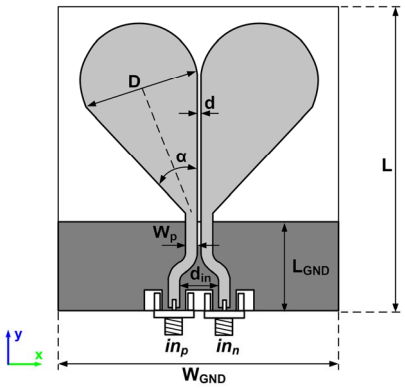


Fig. 2. Layout of the stand-alone UWB antenna. The top copper layer is indicated in light grey. The bottom copper layer is indicated in dark grey.


Fig. 4. Photograph of the stand-alone UWB antenna.

## III. Antenna Performances

Both the board of the radar sensor with the two planar differential UWB antennas and the stand-alone antenna were realized on FR4 substrate, as shown in Figs. 3 and 4, respectively. The simulated performances of the UWB antennas implemented on the radar board of Fig. 3 are reported in Section III-A. The measured and simulated performances of the stand-alone UWB antenna are reported in Section III-B.

### *A. Antenna on the Board of the Radar Sensor*

Simulated $S_{11}$ parameter vs. frequency of the antenna on the board of the radar sensor (see Figs. 1 and 3) is shown in Fig. 5. $|S_{11}|$ is lower than -10 dB in the band of interest from 2.8 to 6.4 GHz. The interest in the lower region of the UWB frequency spectrum is motivated by considering that the energy of the electromagnetic pulses generated by the transmitter is essentially distributed below 5 GHz [6]. Figure 5 reports also the simulation results for the voltage wave standing ratio (VSWR), which is lower than two over the band from 2.8 to 6.5 GHz. The simulated antenna patterns for xz and yz planes, at 3, 4 and 5 GHz are shown in Fig. 6. The plots show also a good coplanar isolation.

TABLE I: Antenna Sizing

| D [cm] | α [deg] | d [mm] | $W_p$ [mm] | $d_{in}$ [cm] | $W_{GND}$ [cm] | $L_{GND}$ [cm] | L [cm] |
|---|---|---|---|---|---|---|---|
| 3 | 45 | 1 | 3 | 1 | 7.1 | 2.3 | 7.9 |

*B. Stand-alone Antenna*

The $S_{11}$ parameter was measured by means of the 20 GHz VNA E5071C by Agilent Technologies®. The differential input of the antenna has been connected to the single ended input of the VNA by means of a wideband 1-12.4 GHz balun by Krytar®. The gain patterns were measured in an anechoic chamber by means of a linearly polarized UWB standard gain horn antenna and an automated positioning system with full rotation angle capability. The setup is shown in Fig. 7. The $S_{11}$ parameter and VSWR resulting from simulations and measurements are shown in Fig. 8. $|S_{11}|$ is lower than -10 dB in the frequency band from about 3 to 5 GHz. Simulated and measured antenna patterns for xz and yz planes, at 3, 4 and 5 GHz, are shown in Fig. 9. The gain is equal to about 2.4 dBi at 4 GHz for theta equal to 0 degrees.

a) b)

Fig. 7. Measurement setup for the experimental characterization of the stand-alone antenna in anechoic chamber. (a) Linearly polarized UWB standard gain horn antenna. (b) Antenna under test on a rotating polystyrene arm. Ferrite chokes were applied on the cables and balun in order to mitigate unwanted interferences.

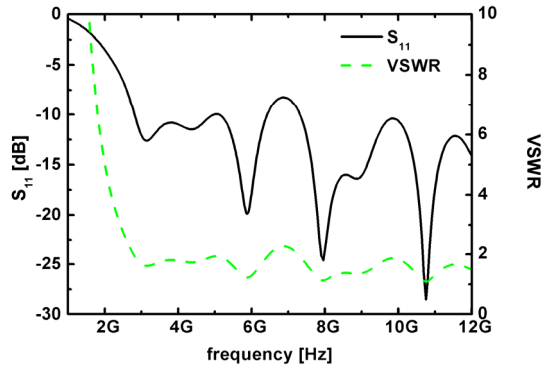


Fig. 5. Simulated $S_{11}$ and VSWR vs. frequency of the antenna on the board of the radar sensor.

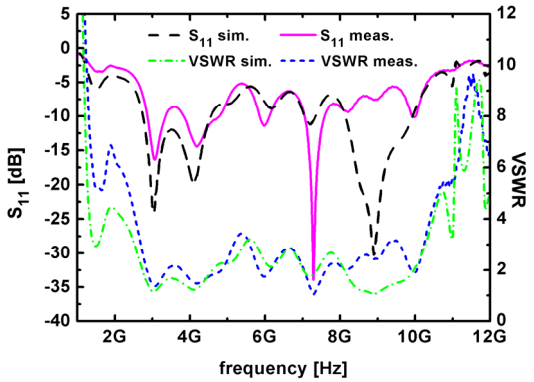


Fig. 8. Measured and simulated $S_{11}$ and VSWR vs. frequency of the stand-alone antenna.

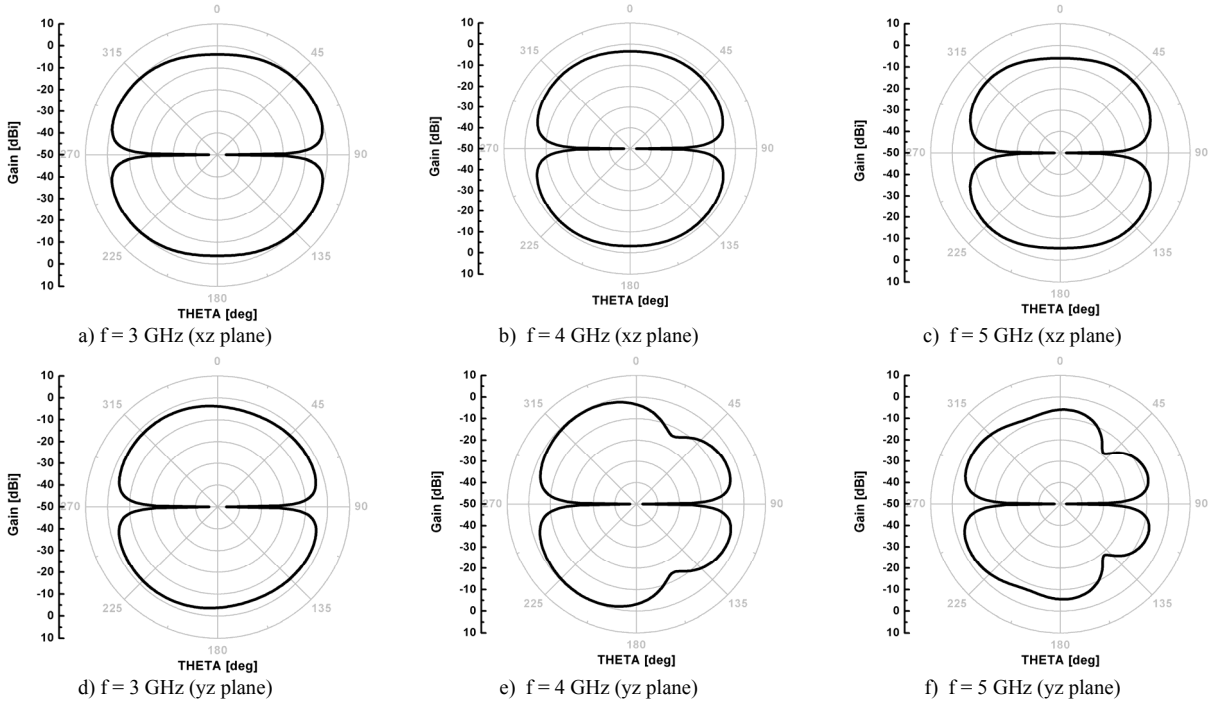


a) f = 3 GHz (xz plane) b) f = 4 GHz (xz plane) c) f = 5 GHz (xz plane)

d) f = 3 GHz (yz plane) e) f = 4 GHz (yz plane) f) f = 5 GHz (yz plane)

Fig. 6. Simulated gain patterns for three different frequencies (3, 4, and 5 GHz), on xz and yz planes of the antenna on the board of the radar sensor.

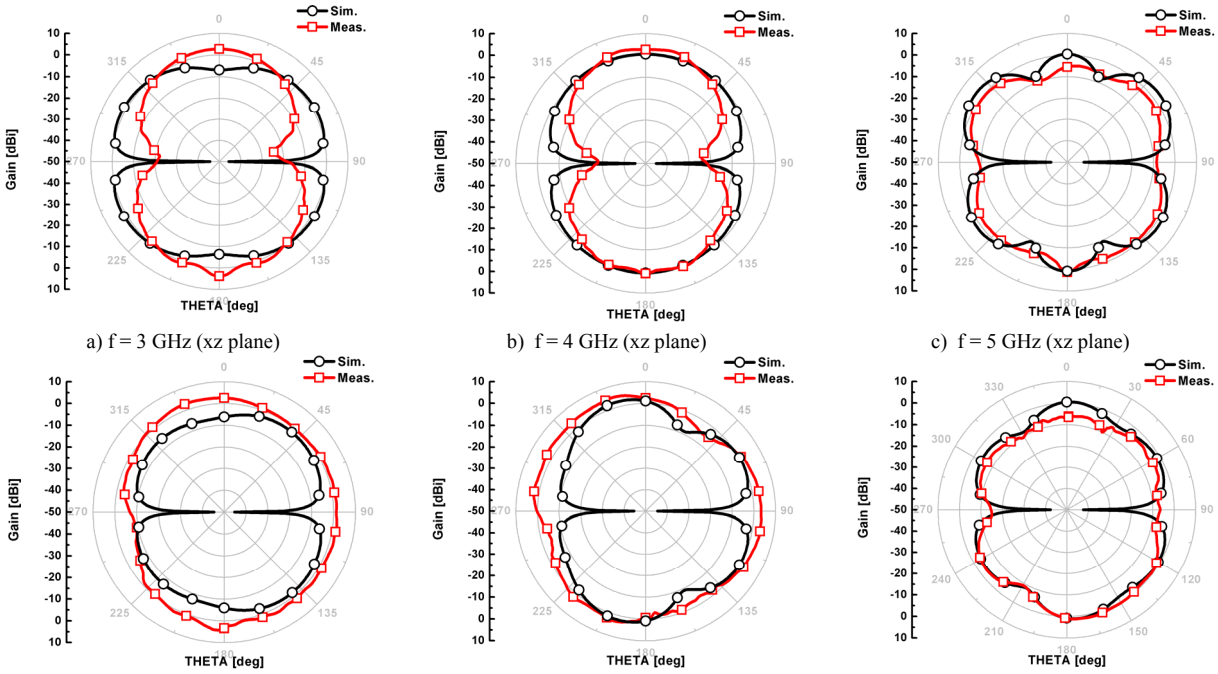


a) f = 3 GHz (xz plane) b) f = 4 GHz (xz plane) c) f = 5 GHz (xz plane)

d) f = 3 GHz (yz plane) e) f = 4 GHz (yz plane) f) f = 5 GHz (yz plane)

Fig. 9. Simulated and measured gain patterns for three different frequencies (3, 4, 5 GHz), on xz and yz planes of the stand-alone antenna.

The SoC radar microchip [2] was attached to the board of the UWB pulse radar sensor with the two antennas (see Fig. 3). Field operational tests carried out in [3] demonstrated that the UWB radar sensor detects correctly sub-centimeter movements of targets (13×13, 13×26 and 26×26 cm) made of plasterboard covered by aluminum foil, as well as the movements of the chest due to the respiratory activity (including apneas) of the person under test, be they adults (both genders) or infants [3]. All the additional details about the field operational tests of the complete radar sensor can be found in [3]. The compliance of the transmitted pulse sequence with the FCC mask is also reported in [3]. The results of the field operational tests reported in [3] validated the effectiveness of the novel UWB planar differential antenna presented herein for the implementation of low-cost UWB pulse radars for short-range applications.

## IV. Conclusions

A planar UWB differential antenna was designed on FR4 substrate to be co-integrated with a SoC UWB pulse radar microchip for short-range applications, including contactless detection of respiratory rate and apneas in adults and infants. In particular, this letter describes in detail the computer-aided design and experimental validation of the antenna as a stand-alone device. It is shown that the resulting UWB antenna is useful for operations in the frequency band from about 3 to 5 GHz. Unlike other planar differential antenna designs, this antenna exhibits a novel topology in which the two sides develop in the same direction (i.e. parallel each other), enabling an effective co-integration with the radar microchip.

The operation of radar sensor was demonstrated through extensive *in-vitro* functional and *in-vivo* field operation tests, including the contactless detection of respiratory rate in adults and infant volunteers, as reported in the cited reference.

## Acknowledgements

The authors are grateful to Agilent Technologies and Microlease for their generous donations of hardware equipment and software computer-aided design tools in support of the research activities carried out at the Marconi Lab established and led by Prof. Domenico Zito.

## References

[1] "New Public Safety Applications and Broadband Internet Access Among Uses Envisioned by FCC Authorization of Ultra-Wideband Technology" FCC, Washington, DC, 2002 [Online]. Available: http://www.fcc.gov/Bureaus/Engineering_Technology/News_Releases/2002/nret0203.html

[2] D. Zito, D. Pepe, M. Mincica, F. Zito, "A 90nm CMOS SoC UWB pulse radar for respiratory rate monitoring", IEEE ISSCC Dig. Tech. Papers, pp. 41-42, Feb. 2011.

[3] D. Zito, D. Pepe, M. Mincica, F. Zito, A. Tognetti, D. De Rossi, "SoC CMOS UWB Pulse Radar Sensor for Contactless Respiratory Rate Monitoring", IEEE Trans. on Biomedical Circuits and Systems, Special Issue on ISSCC 2011, vol. 5, is. 6, pp. 503−510, Dec 2011.

[4] N. Telzhensky, Y. Leviatan, "Planar Differential Elliptical UWB Antenna Optimization", IEEE Transactions on Antennas and Propagation, vol. 54, Is. 11, pp. 3400-3406, Nov. 2006.

[5] H. Nazlı, E. Bıçak, B. Türetken, M. Sezgin, "An Improved Design of Planar Elliptical Dipole Antenna for UWB Applications", IEEE Antennas and Wireless Propagation Letters, vol. 9, pp.264-267, 2010.

[6] F. Zito, D. Pepe, and D. Zito, "UWB CMOS monocycle pulse generator", IEEE Trans. on Circuits and Systems I: Regular Papers, vol. 57, is. 10, pp. 2654−2664, Oct. 2010.

[7] D. Pepe, and D. Zito, "22.7dB gain -19.7dBm iCP1dB UWB CMOS LNA", IEEE Trans. on Circuits and Systems II: Express Briefs, vol. 56, is. 9, pp.689-693, Sept. 2009.